

# Health Estimation and Optimal Operation of a Subsea Gas Compression System Under Uncertainty

Adriaen Verheyleweghen

*Department of Chemical Engineering, Norwegian Univ. of Science and  
technology, Trondheim, NO-7491 (e-mail: verheyle@ntnu.no)*

---

**Abstract:** The efficient and safe operation of subsea gas and oil production systems sets strict requirements to equipment reliability to avoid unplanned breakdowns and costly maintenance interventions. Because of this, condition monitoring techniques are employed to assess the status of the system in real-time. However, the condition of the system is usually not considered explicitly when finding the optimal operation strategy. Instead, operational constraints on flow rates, pressures etc., based on worst-case scenarios, are imposed. This can lead to unnecessarily restrained operation and significant economic losses. To avoid sub-optimal operation, we propose to integrate diagnostics and prognostics with the optimal decision making process for operation to obtain an operational strategy which is optimal subject to the expected system degradation. This allows us to proactively steer the system degradation, rather than simply reacting to it. We use the operation of a subsea gas compressor subject to bearing degradation as a case example.

*Keywords:* Model predictive control, control under uncertainty, diagnostics, prognostics

---

## 1. INTRODUCTION

## 2. BACKGROUND

Subsea processing technology is an enabling technology for fields that were previously deemed too remote; too deep or far away from existing infrastructure. However, several industrial challenges arise when moving topside equipment to the seabed. One of the potentially most prohibitive challenges is the inaccessibility of the plant for large parts of the year, and the need for specialized intervention ships. Consequently, unplanned shut-downs can be very costly and must be avoided as far as possible. In order to achieve this, strict reliability constraints are imposed on design and operation of the plant. While these safety margins provide a method to ensure reliable operation, they might be overly restrictive. One reason for this is because the information from the health monitoring system is often not utilized directly in the decision making process. Instead, a "worst-case" approach is often used to determine production set-points.

In this paper we propose to integrate health monitoring, prognostics and control to obtain a operation strategy that ensures optimal economic profit, but without jeopardizing the plant reliability. In particular, we include a health degradation model in our optimization routine, resulting in a model-predictive control (MPC)-like framework where we impose constraints on the allowable degradation of the equipment. To ensure robustness towards disturbances or uncertainty in the process model, we consider a stochastic optimal control problem. We discretize the uncertainty and solve the resulting multi-stage, scenario-based optimal control problem with direct collocation.

A brief repetition of relevant theory relating to optimization and optimal control is given in this section.

### 2.1 Model predictive control

The MPC principle, which has become popular in industry in recent years due to its ability to deal with constrained, multivariate, and nonlinear control problems, is based on the repeated optimization of the system model, subject to constraints (Morari and Lee, 1999). The first input of the optimized input trajectory is implemented in the plant, before new measurements are taken and the model is re-optimized. For a general differential algebraic equation (DAE) system, the optimal control problem (OCP) which is solved at every time step, can be written as (Biegler, 2010):

$$\min_{x,z,u} \int_0^{t_f} \phi(x,z,u,\pi) dt \quad (1a)$$

$$\text{s.t.} \quad \frac{dx}{dt} = f(x,z,u,\pi) \quad (1b)$$

$$0 = g(x,z,u,\pi) \quad (1c)$$

$$x_L \leq x \leq x_U \quad (1d)$$

$$z_L \leq z \leq z_U \quad (1e)$$

$$u_L \leq u \leq u_U \quad (1f)$$

where  $\phi$  is the objective function,  $x$  denotes the differential states,  $z$  denotes the algebraic states,  $u$  denotes the inputs and  $\pi$  denotes the parameters. Two different classes of methods exist for solving OCPs: direct and indirect methods. While indirect methods give continuous

input profiles, direct methods only provide approximate solutions due to time discretization. Still, direct methods are more commonly encountered due to their ease of implementation and availability of efficient solution algorithms. Direct methods exist in three flavors, depending on how the dynamics are threatened. In single shooting, the entire input profile is integrated at once, starting from some initial state. The drawback is that no information about the states is available to the solver, which can potentially lead to convergence issues if the system is highly non-linear. In multiple shooting, as the name suggests, the system integration is split up into multiple short time intervals. Shooting gaps are added as constraints to make sure that the state trajectories are continuous. The final way of solving OCPs is by using direct collocation, in which the state trajectories are approximated by orthogonal polynomials (Diehl, 2011).

## 2.2 Optimization under uncertainty

When the parameters  $\pi$  are described by a probability distribution  $\xi$  rather than a single value so that  $\pi \in \xi \subset \mathbb{R}^n$ , the optimization problem in (1) becomes a stochastic optimization problem.

$$\min_{x,z,u} \quad \mathbb{E} \left( \int_0^{t_f} \phi(x,z,u,\xi) dt \right) \quad (2a)$$

$$\text{s.t.} \quad c_I(x,z,u,\xi) \leq 0 \quad (2b)$$

$$c_E(x,z,u,\xi) = 0 \quad (2c)$$

where  $\mathbb{E}$  denotes the expectation operator.

With the exception of the case when (2) is an LP, it is generally quite difficult to solve, since it is infinite-dimensional due to the constraints (Birge and Louveaux, 2011). Many approaches for solving stochastic programming problems exist in literature, including worst-case optimization, chance-constrained optimization and scenario-based optimization. In this paper we will use a scenario-based approach to uncertainty. Based on multi-stage stochastic programming, the main idea is to discretize the probability distribution of the uncertain parameter into scenarios. Each scenario represents a path of possible future parameter realizations. Scenarios are bundled together in scenario trees, as shown in Figure 1. Each new branch in the tree represents the possibility of recourse, e.g. the possibility to adjust the inputs in a control setting. While constraint satisfaction can usually not be guaranteed except in the convex case and when the uncertainty set is bounded, the scenario-tree approach performs well for nonlinear systems as well, as long as the nonlinearity is reasonably small (Lucia et al., 2013a).

Due to the exponential growth of the scenario tree with the number of possible parameter realizations at each node, we usually only consider branching up until a point called the branching horizon (Lucia et al., 2013a). The parameters are kept constant after the branching horizon. Since branching represents the availability of new information in the future, shortening the robust horizon means disregarding future state information.

Because decisions can not depend on, or *anticipate*, future realizations of the parameters, it is necessary to include

so-called nonanticipativity constraints. These constraints link together the decisions of scenarios which are branching from a common mother node. For example, the non-anticipativity constraints for the tree in Fig. 1 can be written as

$$u_0^1 = u_0^2 = \dots = u_0^8 = u_0^9 \quad (3)$$

$$u_1^1 = u_1^2 = u_1^3 \quad (4)$$

$$u_1^4 = u_1^5 = u_1^6 \quad (5)$$

$$u_1^7 = u_1^8 = u_1^9 \quad (6)$$

The scenario-based deterministic equivalent of the stochastic OCP reads as

$$\min_{x,z,u} \quad \sum_{i=1}^S p_i \sum_{k=1}^N \phi_k(x,z,u,\pi) \quad (7a)$$

$$\text{s.t.} \quad c_I(x,z,u,\pi) \leq 0 \quad (7b)$$

$$c_E(x,z,u,\pi) = 0 \quad (7c)$$

$$A_{NA}u = 0 \quad (7d)$$

where  $S$  is the number of scenarios,  $N$  is the horizon length,  $p_i$  is the probability associated with scenario  $i$ ,  $\phi$  is the objective function,  $c_I$  and  $c_E$  are the inequality constraints and equality constraints, respectively, and  $A_{NA}$  is the non-anticipativity constraint matrix. Note that we have dropped the subscripts  $i, k$  from the variables  $x, z, u$  and  $\pi$  to avoid cluttering up the notation.

Scenario-based problems often have a high degree of sparsity. Each scenario is one block, with the only thing coupling the blocks together being the nonanticipativity constraints. An illustration of this is shown in Fig. 2. Note the banded structure of the Jacobian of the constraint matrix in Fig. 2. This structure is typical for OCPs, due to the repeated constraints for each stage in the prediction horizon. Similar structure can be seen in the Hessian and consequently the KKT matrix. Problems of this type can be solved rather efficiently in solvers such as IPOPT (Wächter and Biegler, 2006), as they can exploit the sparsity structure of the problem. Furthermore, in the case of stochastic OCPs, the structure can be exploited by dualizing the dynamics and the nonanticipativity constraints. This means that the system is decoupled, and the solver solves many small subproblems (the scenarios) instead of the original, large system. A master problem coordinates the solving of the subproblems and enforces nonanticipativity. This approach also allows for parallelization of the subproblems, which can significantly speed up the calculations.

Creating a scenario tree which captures the true nature of the uncertainty is a difficult task in and of itself. On one hand, the scenario tree should as detailed as possible to be a good approximation of the probability distribution. On the other hand, the scenario tree should be as small as possible due to the curse of dimensionality, which states that the size of the problem, and thereby the computational demand required to solve it, grows rapidly when the number of scenarios is increased. Scenario generation is out of the scope of this paper. We refer the interested reader to Dupačová et al. (2000). In the current work, we do as proposed by Lucia et al. (2013b), which is to generate the scenario tree by using combinations of the

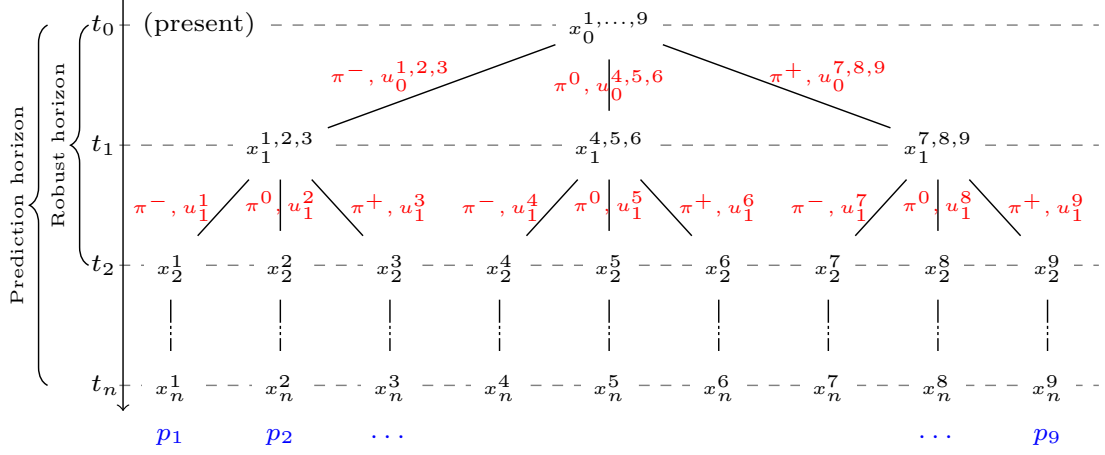


Fig. 1. Scenario tree with prediction horizon  $n$ , robust horizon  $n_{robust} = 2$  and 3 possible parameter realizations ( $\pi^-$ ,  $\pi^0$  and  $\pi^+$ ) at each branching node. Every scenario has an associated probability  $p_i$ .

maximum, minimum, and possibly the nominal uncertain parameters, as identified in the parameter estimation step.

### 2.3 Moving horizon estimation

Moving horizon estimation uses nonlinear programming to estimate states or parameters in DAE systems. Measurements of the system are corrupted by process disturbances  $\omega$  and measurement noise  $\nu$ , both of which are assumed to be unknown. In addition, the system initial state  $x(0)$  is often not known either, making it difficult to say anything about the validity of the measurements and hence the true system state. Luckily, we can compare the measurements to a reference model. By minimizing the least squares error between the measured state and the predicted state, we can estimate the states. The NLP which is solved at each stage in the MHE can be written as (Rawlings and Mayne, 2009, Ch.4)

$$\min_{\hat{x}, \hat{z}, \hat{\pi}, \hat{\omega}, \hat{\nu}} \underbrace{(\chi - \hat{x})^\top P^{-1} (\chi - \hat{x})|_0}_{\text{Arrival cost}} + \underbrace{(\hat{\omega}^\top Q \hat{\omega} + \hat{\nu}^\top R \hat{\nu})}_{\text{Stage cost}} \quad (8a)$$

$$\text{s.t. } c_I(\hat{x}, \hat{z}, u, \hat{\pi}, \hat{\omega}, \hat{\nu}) \leq 0 \quad (8b)$$

$$c_E(\hat{x}, \hat{z}, u, \hat{\pi}, \hat{\omega}, \hat{\nu}) = 0 \quad (8c)$$

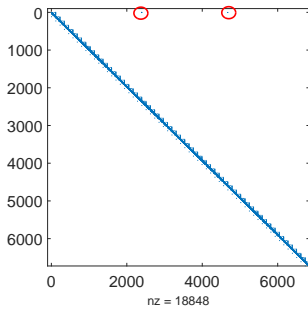


Fig. 2. Sparsity structure of the constraint matrix for a stochastic OCP with prediction horizon  $N = 20$  and 3 scenarios. The coupling constraints are circled in red.

Here, we use hat ( $\hat{\cdot}$ ) notation to indicate the estimates of the corresponding variables.  $P$  is the covariance matrix, while  $Q$  and  $R$  and the weighting matrices for the stage cost.  $\chi$  is the previous estimate of the initial state.

The arrival cost contains information about the confidence level of the initial state prediction, and thus gives a measure about the quality of the state estimates. In this paper, we use the extended Kalman filter (EKF) to calculate the arrival cost. Though more advanced filters, such as particle filters and ensemble Kalman filters exist, these filters will not be used for now. Given the model

$$\frac{dx}{dt} = f(x, u) + \omega \quad (9)$$

$$y = h(x) + \nu, \quad (10)$$

The covariance matrix update equation in EKF can be written as

$$\frac{d\hat{x}}{dt} = f(\hat{x}, u) + K \cdot (y - h(\hat{x})) \quad (11)$$

$$\frac{dP}{dt} = FP + PF^\top - KHP + Q \quad (12)$$

where

$$K = PH^\top R^{-1} \quad (13)$$

$$F = \left. \frac{\partial f}{\partial x} \right|_{\hat{x}, u} \quad (14)$$

$$H = \left. \frac{\partial h}{\partial x} \right|_{\hat{x}} \quad (15)$$

## 3. PROCESS DESCRIPTION

Our case study is a subsea gas compression station, similar to installations on the Åsgard field and the Ormen Lange pilot. The purpose of the gas compression station is to boost the pressure of the stream so that it is sufficiently high to overcome the pressure drop in the transportation pipeline and arrive at the receiving facility topside with the desired outlet pressure. A multiphase boosting pump could be used for this purpose, but since the maturity level of the technology is limited, it is chosen to split the well

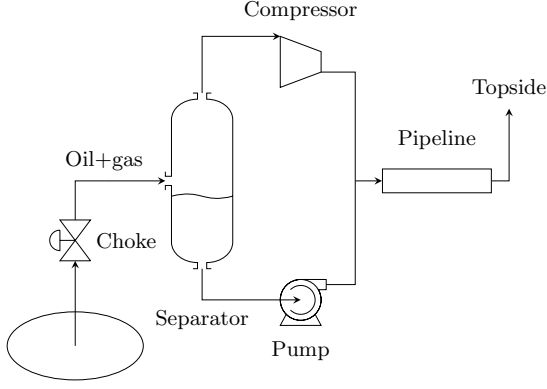


Fig. 3. Subsea gas compression station

stream into its gas and liquid components before increasing the pressure of each sub-stream. An illustration of the process is shown in Figure 3. The system consists of a well choke with which the flow of the hydrocarbons from the reservoir can be controlled. From the reservoir, the stream enters a gas-liquid separator, whose purpose it is to separate the gas from the oil and water. Due to imperfect separation, liquid droplets can be carried over to the gas outlet of the separator. The pressure of the liquid outlet is boosted by a pump before being recombined with the gas. Meanwhile, the pressure of the gas outlet is increased in a compressor. The compressor is modeled as a wet-gas compressor which can handle moderate amounts of liquid carry-over (Aguilera, 2013).

### 3.1 Diagnostics and prognostics

To make meaningful decisions about future production, it is not only necessary to know what the health state of the equipment is at the current time, but one must also be able to predict how the condition of the equipment will develop in the future. Diagnostics is about the detection and monitoring of faults, whereas prognostics is about the prediction of health evolution and estimation of equipment RUL. When talking about a complex system such as a subsea gas compression station, there are potentially hundreds of components which can fail. Since it is not feasible to monitor every single possible point of failure, we chose to monitor only the most vulnerable parts of the system, which for this process are identified to be the bearings in the wet gas compressor. If these bearings were to break down, all operation would have to cease until the broken bearing is replaced. These bearings are subjected to high mechanical stress due to their fast rotational speed, which make them prone to failure.

The health condition of the bearings can be estimated from vibration measurements. We will not go into detail about how this can be done, as it falls outside the scope of the paper. For a full overview, see the (Wang and Kootsookos, 1998). For simplicity, assume that the health state can be measured directly, but that the measurements are corrupted by white noise. Once a fault has been initiated, the bearing will degrade according to Paris' law of crack propagation (Paris and Erdogan, 1963).

## 4. MODEL DESCRIPTION

Below we describe the model used for this work. We assume that the fluid can be described by its gas part and its liquid part. The composition of the fluid is assumed to be constant, and the same in both gas and liquid phase. The thermodynamics of the fluid are mostly ignored, except for necessary properties such as the heat capacity and the compressibility, which are modeled using empirical relationships. The reservoir, the pump and the pipeline are not modeled in this work, but will be included in the future.

### 4.1 Compressor

Since the objective is to ensure reliable operation of the compression station until the next planned maintenance intervention, the timescale of the system is several months. It is therefore reasonable to assume that the dynamics of the flows, temperatures and pressures can be assumed to be instantaneous. Consequently, the only dynamics relevant for this study is the compressor bearing degradation model, which is given by Paris' law.

$$\frac{dx}{dt} = x \cdot c_{Paris} \cdot (Tor^2 \cdot u_{comp.}) \quad (16)$$

$$= x \cdot c_{Paris} \cdot \left( \frac{Pow^2}{u_{comp.}} \right) \quad (17)$$

Here,  $x$  denotes the bearing crack length, i.e. the compressor degradation indicator.  $c_{Paris}$  is a lumped parameter,  $Tor$  is the motor torque and  $Pow$  is the motor power.  $u_{comp.}$  is the shaft frequency, which is a control input. We have assumed that the motor torque can be used as an indicator for gross strain (Bechhoefer et al., 2008).

The compressor is a typical polytropic compressor, which can be described by standard equations found in most textbooks on the topic. For completeness, we repeat the model here.

The polytropic relation is given by

$$\frac{T_{out}}{T_{in}} = \left( \frac{P_{out}}{P_{in}} \right)^{\frac{1}{k}} \quad (18)$$

Where  $k$  is defined in terms of the adiabatic ratios  $\gamma$

$$k = \eta \cdot \frac{\gamma}{1 - \gamma} \quad (19)$$

$$\gamma = \frac{1}{2} \left( \frac{C_{p,in}}{C_{p,in} - R} + \frac{C_{p,out}}{C_{p,out} - R} \right) \quad (20)$$

where  $\eta$  is the compressor efficiency,  $C_p$  is the heat capacity and  $R$  is the gas constant. The heat capacity of a stream is calculated as

$$C_p = (c_1 + c_2 T + c_3 T^2 + c_4 T^{-2}) R \quad (21)$$

The compressor head is

$$H = k \frac{Z_{in} R \cdot (T_{out} - T_{in})}{g M_{in}} \quad (22)$$

$$= \left( c_5 \left( \frac{q_{in}}{u_{comp.}} \right) + c_6 \left( \frac{q_{in}}{den} \right) + c_7 \right) \cdot f_{wood} \quad (23)$$

$$(24)$$

$Z$  is the compressibility factor of the gas,  $g$  is the gravitational constant, and  $M$  is the molar mass. The compressibility factor is calculated using Dranchuk and Abou-Kassem's equation of state (Dranchuk et al., 1975)

$$Z = 1 + \left( A_1 + \frac{A_2}{T_{pr}} + \frac{A_3}{T_{pr}^2} + \frac{A_4}{T_{pr}^3} + \frac{A_5}{T_{pr}^4} \right) \cdot \sigma \\ + \left( A_6 + \frac{A_7}{T_{pr}} + \frac{A_8}{T_{pr}^2} \right) \cdot \sigma^2 - \left( \frac{A_7}{T_{pr}} + \frac{A_8}{T_{pr}^2} \right) \cdot A_9 \cdot \sigma^5 \\ + A_{10} (1 + A_{11} \sigma^2) \left( \frac{\sigma^2}{T_{pr}^3} \right) \exp(-A_{11} \sigma^2) \quad (25)$$

here,  $\sigma$  is

$$\sigma = 0.27 \left( \frac{P_{pr}}{T_{pr}} \right) Z \quad (26)$$

$T_{pr}$  and  $P_{pr}$  denote the pseudo-reduced temperature and pressure, respectively. It can be seen that since  $Z$  in Eq. 25 depends on  $Z$  through  $\sigma$ , which itself depends on  $Z$ , the system of equations describing the model form a semi-implicit index-1 DAE.

$f_{wood}$  is Woods correction factor, which accounts for liquid at the inlet of the wet gas compressor (Hundseid et al., 2008).

$$f_{wood} = \frac{1}{\frac{\rho_{avg}}{\rho_{in}} \sqrt{GVF_{in} \cdot \frac{\rho_{avg}}{\rho_{in}}}} \quad (27)$$

The average density of the inlet is

$$\rho_{avg} = GVF_{in} \cdot \rho_{in} + (1 - GVF_{in}) \rho_{cond}. \quad (28)$$

where  $GVF$  is the gas volume fraction of the stream and  $\rho_{cond.}$  is the density of condensate. The compressor power can be found from the energy balance

$$Pow = \frac{H q_{in} \rho_{in} g}{\eta} \quad (29)$$

Here, we use  $q$  to denote the volumetric gas flow. Furthermore, we need to define two variables,  $Srg$  and  $Stw$  which indicate surge and Stonewall conditions (compressor choking), respectively. Values less than zero indicate either compressor surging or choking, which are both undesired phenomena.

$$Srg = H + c_8 q_{in}^2 + c_9 q_{in} + c_{10} \quad (30)$$

$$Stw = H + c_{11} q_{in}^2 + c_{12} q_{in} + c_{13} \quad (31)$$

Finally, we need to express the efficiency  $\eta$  in terms of the gas volumetric flow and the compressor speed as

$$\eta = f(q_{in}, u_{comp.}) \quad (32)$$

The function  $f$  is given by the compressor map, which is unique to each compressor. We use a polynomial fit of the compressor map from Aguilera (2013).

#### 4.2 Choke

Opening and closing the choke adjusts the flow into the separator. The flow through the choke is given by the valve equation

$$m = u_{choke} c_{choke} \sqrt{P_{in} - P_{out}} \quad (33)$$

where  $c_{choke}$  is the choke constant, and  $u_{choke}$  is the choke opening. The mass flow relates to the volume flow through

$$m = q \rho \quad (34)$$

and to the gas-volume-fraction as

$$GVF = \frac{q_{gas}}{q_{gas} + q_{cond.}} \quad (35)$$

#### 4.3 Separator

The separator splits gas and condensate into separate streams. The separator efficiency is modeled as a function of the gas velocity and the fluid density (Austheim, 2006). The separation efficiency  $\alpha$  is given by

$$\alpha = 1 - \frac{\rho_{gas}^2}{c_{14}} - c_{15} \rho_{gas}^2 K^3 \quad (36)$$

where  $K$  is

$$K = \frac{q}{A} \sqrt{\frac{\rho_{gas}}{\rho_{cond.} - \rho_{gas}}} \quad (37)$$

$A$  is the cross-sectional area of the separator.

#### 4.4 Model summary

The model describing the gas compression system is a semi-implicit index-1 DAE with one differential state and 36 algebraic states. Two control inputs are available, namely the choke opening  $u_{choke}$  and the compressor speed  $u_{comp.}$ .

### 5. DEFINING THE OCP

The objective of the controller is to achieve economically optimal operation, subject to health constraints. The objective function is

$$\min_{x,z,u} \mathbb{E}_\xi \int_0^{t_f} \left( -\frac{m_{gas}(x,z,u,\xi)}{(1+r)^t} \right) dt \quad (38)$$

where the discount factor  $r = 0.015$ . The deterministic equivalent objective function is

$$\min_{x,z,u} \sum_{i=1}^S \sum_{k=1}^N \left( -\frac{m_{gas}(x,z,u,\pi)}{(1+r)^{t_k}} \right) \quad (39a)$$

The variable bounds are

$$0.75 \leq u_{comp.} \leq 1.05 \quad (40)$$

$$0 \leq u_{choke} \leq 1 \quad (41)$$

$$0 \leq x \leq 1 \quad (42)$$

$$0 \leq Srg \quad (43)$$

$$0 \leq Stw \quad (44)$$

$$150 \text{ bar} \leq P_{out} \quad (45)$$

$$x(0) = x_0 \quad (46)$$

The constraints on  $Srg$  and  $Stw$  are added to limit operation to the allowable operating region, while the constraint on  $P_{out}$  is imposed after the compressor to ensure flow through the long pipeline to the topside. The initial condition  $x_0$  of the OCP is the estimated state  $\hat{x}(0)$  from the MHE step.

Since the problem is a DAE with constraints on the algebraic states, we chose to solve the OCP with direct collocation with a Radau scheme. It would be possible to solve the problem using multiple shooting with an implicit integrator as well, but we would have to force the integrator to report the algebraic states in order to impose constraints on them. We solve the problem in a shrinking-horizon manner, starting with an initial prediction horizon of  $N = 20$  with  $d = 3$  Radau points on each finite element.

The parameter  $c_{Paris}$  in the crack propagation model from Eq.(16), and the gas volume fraction in the reservoir  $GVF$ , are assumed to be uncertain. The possible realizations of the uncertain variables are given in Tab. 1. The possible

Table 1. Values of the uncertain variables  $c_{Paris}$  and  $GVF$  in the scenarios.

Parameter	High	Low	Mean
$c_{Paris}$	1.10	0.90	1.00
$GVF$	0.92	0.88	0.90

realizations of the variables are combined to form the scenarios for the scenario tree. The first stage has five branches, being the extreme realizations and the mean. Each of those branches splits into nine more branches, this time being all possible combinations of the realizations. The scenario tree thus consists of 45 scenarios, and has a robust horizon of  $n_{robust} = 2$ .

## 6. DEFINING THE MHE

The moving horizon estimator is used to estimate the health state  $x$  from the noisy measurements, and the parameter  $c_{Paris}$ . The estimator uses a reduced order model of the system. We assume that measurements of  $Pow$  are available, so that Eq. (16) can be used directly to estimate the variables. The MHE model is therefore a pure ODE with one differential state.

The weights for  $Q$  and  $R$  are based on trial and error. It was found that

$$R = \text{diag}(0.02^2) \quad (47)$$

$$Q = \text{diag}(0.03^2, 0.03^2) \quad (48)$$

gave satisfactory performance.

## 7. RESULTS

Both the stochastic MPC and the MHE were implemented in MATLAB using Casadi 3.0.0 (Andersson, 2013) and solved using IPOPT 3.12.3 (Biegler, 2010) with MUMPS as linear solver.

At time  $t = 0$  a crack of length  $x_0 = 0.01$  is initiated. The estimator is initiated at  $\hat{x}_0 = [0.0 \ 1.5]^T$ , and  $P_0 = I$ . The MHE was initialized with a vector of measurements around  $\hat{x}_0$ , with added white noise. At  $t = 2.5$ , the  $GVF$  is changed from 0.9 to 0.92, to simulate a change in the reservoir conditions. The closed-loop solution of the health-aware controller with a maintenance horizon of 5 years is shown in Fig. 4. The corresponding state and parameter estimates from the MHE are shown in Fig. 5.

The results seem logical. It can be seen that the gas production rate is high in the beginning and decreases over time. This is caused by the NPV term in this cost function, which favors early gas production over late gas production. The optimal solution in absence of uncertainty is to maximize the gas production while keeping the outlet pressure constraint active, in order to avoid costly over-compression of the gas, as this will degrade the compressor faster. One can think of this strategy as using the compressor to control the outlet pressure and using

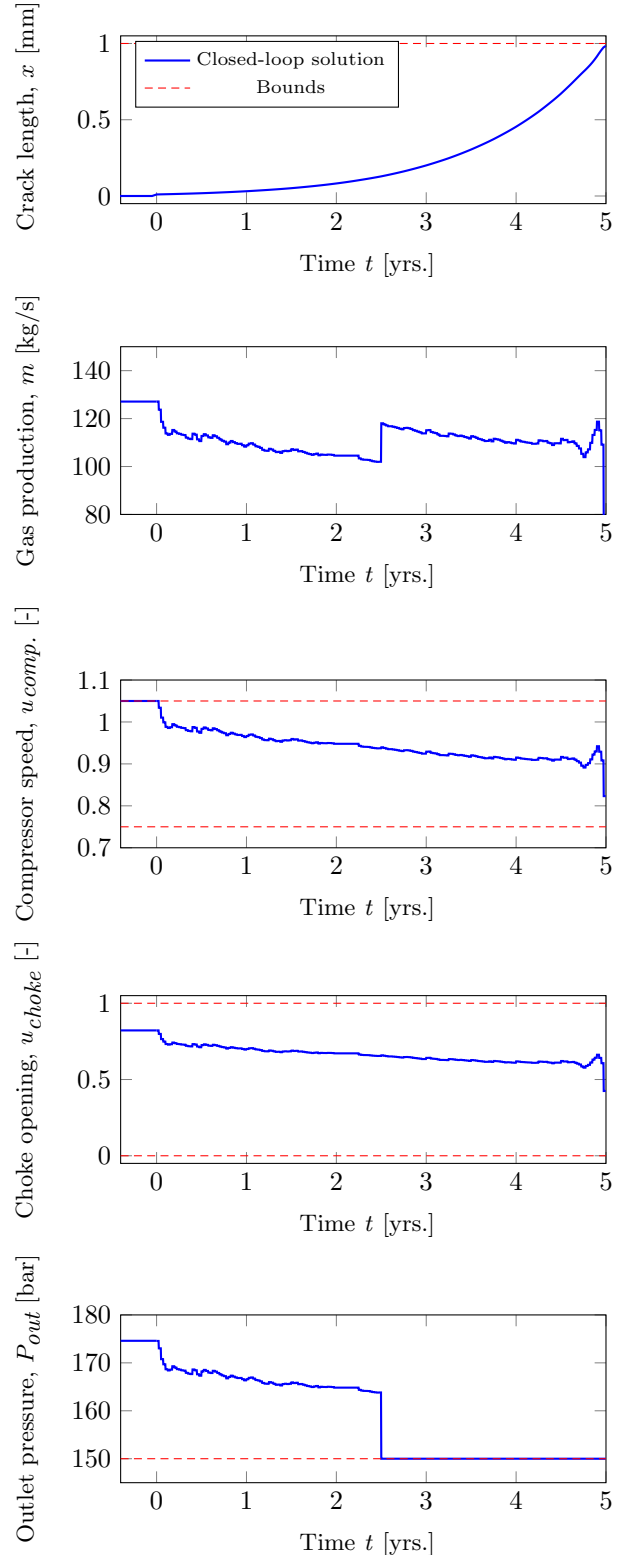


Fig. 4. Closed loop profiles of the controlled variables and the inputs. The state profiles are shown in blue and the constraints are shown in red.

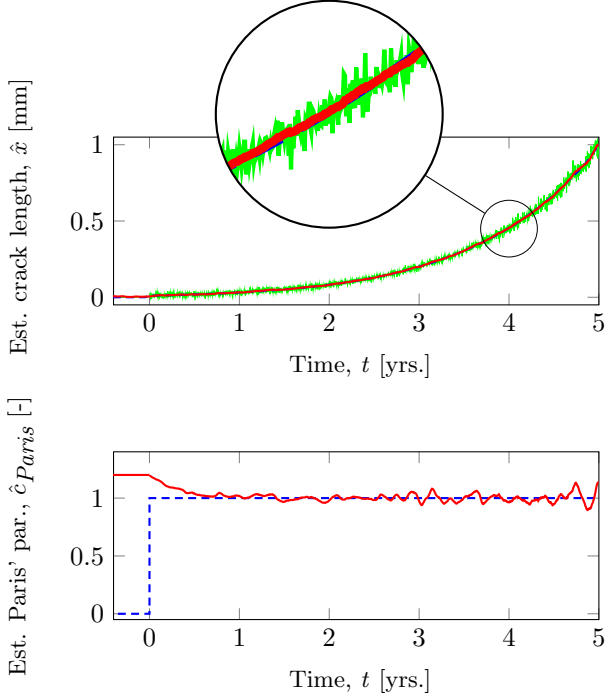


Fig. 5. Closed-loop results of the moving horizon estimator. The estimates are shown in red, the true states are shown in blue, and the noisy measurements are shown in green.

the choke to control the production profile such that the health constraint is not violated. It can be seen that in the presence of uncertainty, the optimal strategy is to back off from the pressure constraint to account for possible variations in the *GVF*. When the change in *GVF* occurs at  $t = 2.5$ , the outlet pressure constraint becomes active. Even in the presence of uncertainty, the maximum allowable degradation constraint is not violated. Towards the end of the horizon, the controller realizes that the health constraint will hold, and it tries to squeeze more gas production out of the system by briefly increasing the inputs.

The moving horizon estimator tracks the states relatively closely. The non-linearities from one sample time to the next are not very large, so the EKF does a reasonable job at propagating the state covariance matrix and initial state estimates. It can be seen in Fig. 8 that the state  $x$  is tracked very closely. The parameter estimate  $\hat{c}_{Paris}$  is decent, but could most likely be improved by adjusting the tuning parameters in the MHE, or by using more samples at each stage. Currently, the estimator has a prediction horizon of 30 samples, which might be too short to capture the dynamics of the system. Towards the end of the horizon, the estimates become worse because the noise level is increasing (the noise is proportional to the state).

## 8. DISCUSSION

The success of our proposed approach hinges on the quality of the degradation model and condition monitoring capabilities. Our approach relies on the equipment vendors to provide models and data for performing the diagnostics and prognostics. Since the objective of this paper is to

demonstrate our method, we have chosen to use a relative simple degradation and diagnostics model, that we adapted to our purposes.

Scenario-based approaches are robust to uncertainties / disturbances, as long as their set of possible realizations is captured reasonably well by the scenario tree approximation. One might be tempted to model all variables in terms of their probability distributions, but this would lead to a large number of scenarios, which would become intractable to solve in reasonable time. Indeed, we observed slow convergence already at 45 scenarios, which is a small number of scenarios in the context of stochastic optimization (Birge and Louveaux, 2011). While warm-starting somewhat helped to speed up convergence, the interior point method employed by IPOPT does not really utilize warm-starting as well as an SQP-based solver would (Diehl, 2011). Even though sparsity of the stochastic program can be exploited by the solver, decomposition (via Lagrangian relaxation (Nowak and Römisch, 2000)) and parallelization are necessary to increase the number of scenarios even further while keeping the computational time down. While computational time is not a major issue for the implementation, since the time constant is measured in years, it is desirable to have fast convergence when prototyping.

On the other hand, the number of scenarios can be reduced by shortening the robust horizon. We observed that increasing the robust horizon beyond 1 gave diminishing returns at the cost of a much larger NLP. Due to the frequent re-optimization of the problem, the added value of additional branching is negligible.

It should also be mentioned that disturbance rejection, as shown here for a disturbance in *GVF* should be handled at the underlying control layer, rather than at the "scheduling" layer considered here. A multi-layer approach will be investigated in the future. For now, we included a disturbance in *GVF* to show that the scenario-based approach is robust towards unmeasured disturbances as well, as long as they are included in the scenario tree.

## 9. CONCLUSION AND FUTURE WORK

We showed how prognostics and control can be combined to a subsea gas compression plant subject to compressor bearing failure. By including measurements of fault indicators and fault prognostic models in the MPC framework, we can ensure that the operation is both economically optimal and safe. Disturbances and uncertainty in the degradation model are handled explicitly by formulating a scenario-based shrinking horizon MPC.

In future work, we will consider multiple failure mechanisms, not only bearing failures. Furthermore, we will look at the possibility of including more scenarios by using decomposition and parallelization to handle the larger NLP. We would also like to look at methods to solve the problem to global optimality, since this is an important aspect when considering reliability.

## REFERENCES

- Aguilera, L.C.P. (2013). *Subsea Wet Gas Compressor Dynamics*. Master's thesis, Norwegian University of Science and Technology.

- Andersson, J. (2013). *A General-Purpose Software Framework for Dynamic Optimization*. PhD thesis, Arenberg Doctoral School, KU Leuven, Department of Electrical Engineering (ESAT/SCD) and Optimization in Engineering Center, Kasteelpark Arenberg 10, 3001-Heverlee, Belgium.
- Austrheim, T. (2006). *Experimental Characterization of High-pressure Natural Gas Scrubbers*. Ph.D. thesis, University of Bergen.
- Bechhoefer, E., Bernhard, A., and He, D. (2008). Use of paris law for prediction of component remaining life. In *Aerospace Conference, 2008 IEEE*, 1–9. IEEE.
- Biegler, L.T. (2010). *Nonlinear programming: concepts, algorithms, and applications to chemical processes*, volume 10. SIAM.
- Birge, J.R. and Louveaux, F. (2011). *Introduction to stochastic programming*. Springer Science & Business Media.
- Diehl, M. (2011). Numerical optimal control. *Optimization in Engineering Center (OPTEC)*.
- Dranchuk, P., Abou-Kassem, H., et al. (1975). Calculation of z factors for natural gases using equations of state. *Journal of Canadian Petroleum Technology*, 14(03).
- Dupačová, J., Consigli, G., and Wallace, S.W. (2000). Scenarios for multistage stochastic programs. *Annals of operations research*, 100(1-4), 25–53.
- Hundseid, O., Bakken, L.E., Gruner, T.G., Brenne, L., and Bjorge, T. (2008). Wet gas performance of a single stage centrifugal compressor. In *ASME Turbo Expo 2008: Power for Land, Sea, and Air*, 661–670. American Society of Mechanical Engineers.
- Lucia, S., Finkler, T., and Engell, S. (2013a). Multi-stage nonlinear model predictive control applied to a semi-batch polymerization reactor under uncertainty. *Journal of Process Control*, 23(9), 1306–1319.
- Lucia, S., Subramanian, S., and Engell, S. (2013b). Non-conservative robust nonlinear model predictive control via scenario decomposition. In *Control Applications (CCA), 2013 IEEE International Conference on*, 586–591. IEEE.
- Morari, M. and Lee, J.H. (1999). Model predictive control: past, present and future. *Computers & Chemical Engineering*, 23(4), 667–682.
- Nowak, M.P. and Römisch, W. (2000). Stochastic lagrangian relaxation applied to power scheduling in a hydro-thermal system under uncertainty. *Annals of Operations Research*, 100(1-4), 251–272.
- Paris, P. and Erdogan, F. (1963). A critical analysis of crack propagation laws. *Journal of basic engineering*, 85(4), 528–533.
- Rawlings, J.B. and Mayne, D.Q. (2009). *Model predictive control: Theory and design*. Nob Hill Pub.
- Wächter, A. and Biegler, L.T. (2006). On the implementation of an interior-point filter line-search algorithm for large-scale nonlinear programming. *Mathematical programming*, 106(1), 25–57.
- Wang, Y.F. and Kootsookos, P.J. (1998). Modeling of low shaft speed bearing faults for condition monitoring. *Mechanical Systems and Signal Processing*, 12(3), 415–426.